Molecular Crystals and Liquid Crystals Science and Technology. Section A. Molecular Crystals and Liquid Crystals

Publication details, including instructions for authors and subscription information:
http://www.tandfonline.com/loi/gmcl19

The X-Ray Crystal Structures and Computational Analysis of NH…π Hydrogen Bonded Banana-Shaped Carbazole Derivatives and Thermal Analysis of Higher Mesogenic Homologues

Maura Belloni [a], M. Manickam [a], Peter R. Ashton [a], Benson M. Kariuki [a], Jon A. Preece [a], Neil Spencer [a] & John Wilkie [a]

[a] School of Chemistry, University of Birmingham, Edgbaston, Birmingham, B15 2TT, (UK)

Version of record first published: 24 Sep 2006

To cite this article: Maura Belloni, M. Manickam, Peter R. Ashton, Benson M. Kariuki, Jon A. Preece, Neil Spencer & John Wilkie (2001): The X-Ray Crystal Structures and Computational Analysis of NH…π Hydrogen Bonded Banana-Shaped Carbazole Derivatives and Thermal Analysis of Higher Mesogenic Homologues, Molecular Crystals and Liquid Crystals Science and Technology. Section A. Molecular Crystals and Liquid Crystals, 369:1, 17-35

To link to this article: http://dx.doi.org/10.1080/10587250108030006

Mol. Cryst. Liq. Cryst., Vol. 369, pp. 17-35
Reprints available directly from the publisher
Photocopying permitted by license only

The X-Ray Crystal Structures and Computational Analysis of NH...π Hydrogen Bonded Banana-Shaped Carbazole Derivatives and Thermal Analysis of Higher Mesogenic Homologues

MAURA BELLONI, M. MANICKAM, PETER R. ASHTON, BENSON M. KARIUKI, JON A. PREECE*, NEIL SPENCER and JOHN WILKIE

School of Chemistry, University of Birmingham, Edgbaston, Birmingham B15 2TT (UK)

(Received November 6, 2000; Revised December 15, 2000)

The synthesis of a series of banana-shaped mesogenic structures has been carried out, in which the bend unit is formed by the 3,6-substitution of carbazole by 4-alkoxyphenyl moieties. The crystal structures of the methoxy and propyloxy derivatives are reported with an analysis of the N-H···π interactions that are observed in the crystalline state. This analysis was aided by semi-empirical molecular orbital calculations. Additionally, the thermal analysis of the complete series has been carried out in order to investigate the phase properties of these materials. The 4-nonyloxyphenyl derivative displays two melting points by DSC and normal light microscopy, but yields non-birefringent liquids. The incorporation of photorefractive molecular units, such as carbazole, into anisotropic materials may offer many advantages over conventional electrical poling of photorefractive polymers.

Keywords: Banana; carbazole; N-H···π hydrogen bonding; liquid crystals

INTRODUCTION

Due to their extensive biological activity carbazole derivatives and their chemistry have been studied at length.[1] However, it is only recently that they have been studied in terms of their material properties[1,2] and in particular their pho-

* Corresponding Author: Telefax: Int. code +121 414 4403, E-mail: j.a.preece@bham.ac.uk

torefractive properties.[3] The interest in photorefractive materials[4] lies in their numerous potential technological applications,[5] such as high density optical data storage, optical image processing, phase conjugated mirrors, dynamic holography, optical computing, parallel optical logic, and pattern recognition. Thus, recent studies on carbazole materials have been concerned with electroluminescence,[6] nonlinear optics,[7] and photoconductivity.[8] Amorphous organic photorefractive materials[9] have many advantages over crystalline inorganic[3] and latterly crystalline organic[10] photorefactive materials on which the early research was carried out. These advantages include large optical nonlinearities, low dielectric constants, low cost, structural flexibilty, and ease of fabrication. However, the major drawback of the amorphous organic photorefractive materials is that a low $T_g$is required in order that the material can be aligned by a dc electric field to induce a degree of anisotropic ordering.[11] The chemical modification of the carbazole moiety to induce liquid crystallinity is attractive in order to combine the advantages of the amorphous materials with anisotropic ordering. However, to date there are only a few examples in which the carbazole moiety has been incorporated into thermotropic low molecular weight calamitic and polymeric liquid[12] crystalline materials and into a lyotropic phase[13] but no examples of discotic,[14] chiral,[15] or banana[16] liquid crystals containing the carbazole moiety which may display, in the case of the latter two, the important ferroclectric switching mesophase.[17] Thus, we have recently reported the first low molecular weight thermotropic hexagonal columnar discotic liquid crystals which incorporate the carbazole moiety.[18] Here we report a programme of research which aims to create novel carbazole based liquid crystals which exploits the molecular structure of the carbazole to afford banana-shaped mesogenic materials. In particular, we highlight (i) our molecular design requirements, (ii) the synthesis of our first generation of banana-shaped mesogenic structures, (iii) the crystal structure of two of our banana-shaped carbazole compounds, (iv) a simple computational analysis of the hydrogen bonding interactions observed in two of the compounds in the crystalline state, and (v) the phase behaviour of the materials as a function of temperature.

RESULTS AND DISCUSSION

Design

The target structure that was designed is shown in Figure 1, where the 3 and 6 positions of the carbazole moiety have been chemically modified by the substitu-

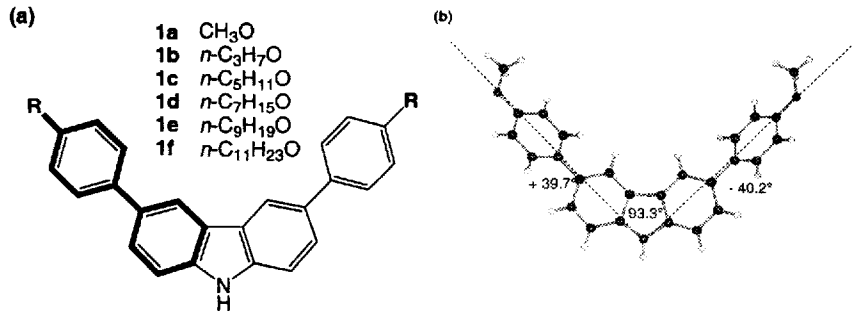

FIGURE 1 Target carbazole bent molecular structures **1a-f** and the crystal structure of **1a**, highlighting the pseudo C_2v symmetry

tion of the hydrogen atoms with 4-alkoxyphenyl moieties, resulting in structures **1a-f**. This generic structure appears to fulfil the criteria of a bent molecular structure with C_2v symmetry as well as incorporating mesogenic alkyloxybiphenyl moieties (highlighted in bold bonds). However, the banana-shaped molecular structures which have been reported to date which display mesophases, generally, have a central 1,3-disubstituted benzene central unit affording the bend[19] and two[20] or three[21] para substituted phenyl units linked directly or via ester[22] or imine[23] linkages to the central unit. Thus, the literature structures have 5–7 independent phenyl ring structures. In our design we have 5 rings but three of these are fused in the carbazole moiety, and the central ring is a heteroaromatic ring. However, recently banana shaped molecules which display mesophases have been reported which contain fused ring systems (2,7 naphthalene moiety[21]), as well as heteroaromatic systems (2,5-thiophene[24] and 2,6-pyridine[21]) as the bend unit. But it should be noted that of the banana-shaped mesogens which display mesophase, very few display the ferroelectric B_2 mesophase.[25]

Synthesis

The chemistry of carbazole allies it very well to being the "bent" component in banana structures because the pyrrolic nitrogen atom directs electrophilic aromatic substitution to the 3 and 6 positions, affording the bent architecture. Thus, our synthesis relies upon the electrophilic aromatic substitution of the 3 and 6 carbazole hydrogen atoms with bromine atoms to afford the 3,6-dibromocarbazole derivative **2**. The dibromo derivative is subsequently reacted with a homologous series of 4-alkoxyphenyl boronic acids **3a-f** to afford the target compounds

1a-f. The boronic acid derivatives are formed from an initial alkylation of 4-bromophenol with appropriate alkyl halides to afford **4a-f**, which are subsequently reacted with butyllithium and trimethyl borate and quenched with aqueous HCl to afford the desired boronic acids **3a-f**.

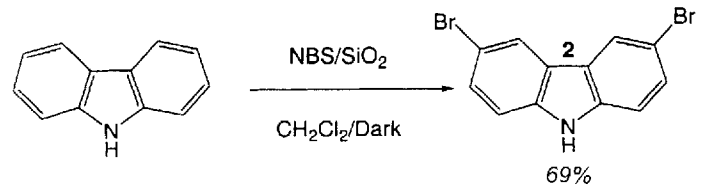

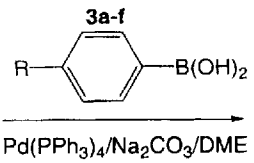

Target Compounds (Figure 1a)

	R	Yield/%
1a	CH_3O	*60*
1b	n-C_3H_7O	*50*
1c	n-$C_5H_{11}O$	*50*
1d	n-$C_7H_{15}O$	*28*
1e	n-$C_9H_{19}O$	*40*
1f	n-$C_{11}H_{23}O$	*53*

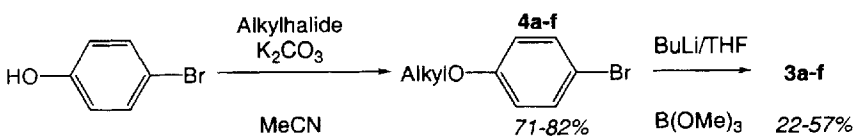

SCHEME Synthesis of the carbazole derivatives **1a-f**

Crystal Structures

In the crystal structure of **1a**, the 3,6 substitution on the carbazole moiety results in an exocyclic bond angle of 93.3° (Figure 1b). The two phenyl rings are twisted out of the plane of the carbazole moiety by +39.7° and −40.2° resulting in pseudo C_2v molecular symmetry. The $\underline{C}H_3$-O-C_{ar} atoms are coplanar to the carbon atoms of the phenyl rings they are bonded to. In the crystal (Figure 2a(i)), N-H···π interactions[26] are observed between neighbouring molecules, utilising the pyrolle moiety of the carbazole unit as the π-base. This results in hydrogen bonded chains along the b axis, in which **1a** is both a H-bond donor and a H-bond acceptor (π-base), leading to a herringbone type packing arrangement. The distance between the proton and the middle of the pyrrole ring is 2.87 Å. Parallel chains are stacked along the a axis to form sheets in the ab plane (Figure 2a(ii)).

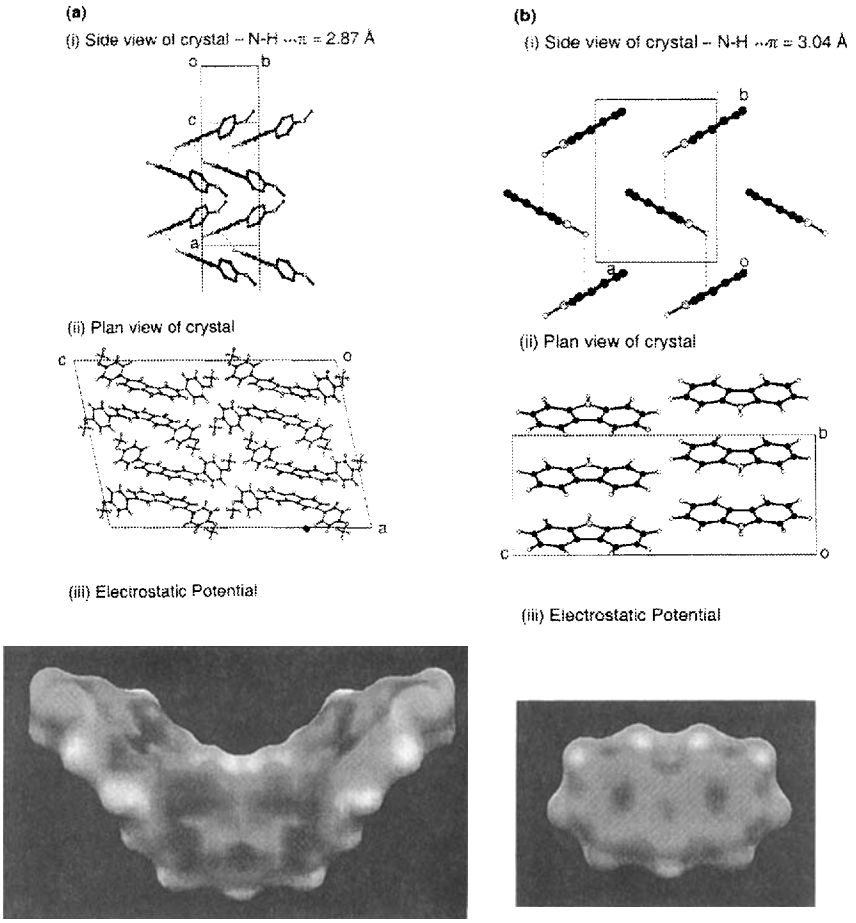

FIGURE 2 Ball and stick representation of the packing of molecules in the crystalline state of **1a** (a(i) and a(ii)) and carbazole (b(i) and b(ii)), the electronic distribution structure of **1a** (a-iii) and carbazole (b-iii) (darker shade represents increasing electron density). Note the common sheet like-herringbone packing of both structures, but contrast the *anti* and *syn* ordering of adjacent molecules as viewed from the top to the bottom of the page in both structures, respectively. However, the crystal of **1a** is still a centrosymmetric structure by virtue of the anti packing of adjacent sheets of molecules

The NH···π chains are antiparrallel in neighbouring sheets leading to an overall centrosymmetric crystal packing. The methoxy oxygen atoms are not involved in NH···O hydrogen bonding.

The structure of **1a** displays similarities with that of carbazole[27] which also has chains of molecules linked by NH···π interactions (Figure 2b(i)). The chains are stacked to form antiparallel sheets comparable to those in **1a** (Figure 2b(ii)),

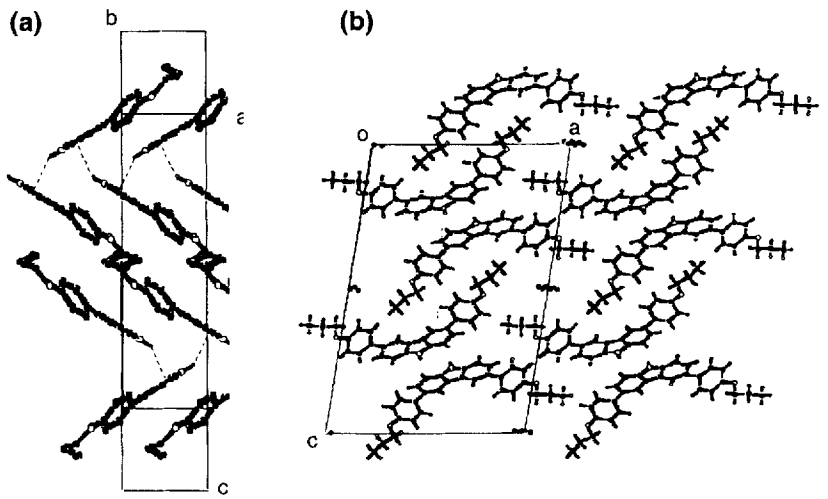

FIGURE 3 Ball and stick representation of the packing of molecules in the crystalline state of **1b** illustrating (a) the chains of molecules linked by hydrogen bonds and (b) the offset nature of the carbazole moeities, relative to structure **1a** and carbazole, resulting in channels incorporating solvent molecules

again leading to a herringbone structure packing motif. However, in carbazole, the NH···π distances in the chains are longer (3.04 Å), an aspect which we investigate by computational methods below. Another difference is the nearly *anti* alignment of neighbouring molecules in carbazole compared to the *syn* arrangement in **1a**. Neither structure displays π- π interactions.

The structure of **1b** was also determined. This revealed that the two phenyl rings in the molecule are twisted also out of the plane of the carbazole fragment by +30.2° and −30.7° (10° less than in **1a**). NH···π interactions are also observed in **1b** but the N-H bond is directed towards one of the non-heterocyclic rings of the carbazole moiety and not the pyrrole moiety as in **1a** (Figure 3a). This NH···π interaction is not as dominating as evidenced by the longer bond length of 3.07Å. Again, as with **1a** and carbazole the NH···π interaction leads to hydrogen bonded chains along the a axis. We assume the NH···π interaction is directed to the non-heterocyclic π-unit of the carbazole as a result of structural packing arrangements dominating over the electrostatics, because the electrostatic potential of both heterocyclic and non-heterocyclic π-units in the carbazole moiety of **1a** (and **1b**) are very similar (see computational methods). The chains of molecules are stacked in an antiparallel manner with slight offsets in order to accommodate the bulkier propyloxy groups, but again the herringbone type packing arrange-

ment is maintained. This offset creates channels which are occupied by disordered solvent molecules (Figure 3b). Both propyloxy groups in the molecule are also disordered, an aspect which we desire in order to attain the balance between order/disorder in our materials to induce mesophases.

Computational Chemistry

In order to try and understand the differences and similarities in the two crystal structures of **1a** and carbazole we have utilised computational chemistry to model the electrostatics of single molecules of **1a** and carbazole (Figure 2a(iii) and 2b(iii), respectively). The semi-empirical molecular orbital calculations readily reproduce the 40° twist of the phenyl rings observed in the crystal structure (Figure 2a(iii)) and reveal that the nett out-of-π-plane$_{carbazole}$ dipole is a combination of an in π-plane$_{carbazole}$ dipole and an orthogonal out-of π-plane$_{carbazole}$ dipole (resulting from out of π-plane$_{carbazole}$ O-Me units). Semi-empirical molecular orbital theory calculations reveal that **1a** has a larger nett dipole than carbazole, the values being 2.878 and 1.206 D, respectively. Considering the electrostatic potential of isolated molecules, both **1a** and carbazole have similar electrostatic potentials over the bonded N-H atoms (carbazole N = –0.5414, H = +0.4066; **1a** N = –0.5374 H = +0.4051). However, the electrostatic potential of the pyrrole component of the carbazole moiety is a factor of 4 more negative in **1a** than in carbazole (Figure 2a(iii) and 2b(iii)). The non-heterocyclic π-unit in the carbazole moiety of **1a** has a comparable electrostatic potential to the pyrrolic moiety. Furthermore, the calculated proton affinity for **1a** is 334 kJ mol^{-1}, whilst for carbazole it is 341 kJ mol^{-1}. Thus, we conclude that the hydrogen bond length in **1a** is shorter than in carbazole as a consequence of at least two factors; (i) the pyrrole moiety in **1a** is a stronger π-base, and (ii) the proton in **1a** is more acidic.

Phase Behaviour

The DSC traces of **1a-e** are illustrated in Figure 4. It is clear and expected that for **1a** and **1b** there is a clear isotropic melting transition from the crystalline state at 214.6°C and 175.7°C, respectively. For **1c** the DSC is rather more complicated but we have interpreted this as some polymorphic transitions followed by isotropic melting at 129.5°C, but clearly there is no evidence of any mesophase. The DSC analysis of **1d** shows an exotherm at 123.0°C and isotropic melting at 124.6°C. However, the DSC analysis of **1e** hints that this may be a mesophase forming material, where a large endotherm is observed at 117.1°C and a smaller

one at 127.2°C, suggesting melting to an anisotropic liquid and subsequent isotropisation. However, observation of **1e** between crossed polarisers as the sample was both heated to isotropisation and cooled to the crystalline state did not reveal any birefringent liquid. Normal optical light microscopy revealed that the material did appear to have two melting points; firstly from the solid to a clear viscous oil and then to a non-viscous liquid. It should be noted that elemental analysis and HPLC analysis of this compound indicates that the material is pure(>99.9%). Thus, at this stage we are not clear as to the exact liquid phases of this material. The DSC analysis of **1f** shows two very close endotherms of comparable magnitude at 74.5°C and 77.7°C, respectively. It should be noted that all materials (**1a-f**) when observed under the optical polarising microscope revealed melting from solid to nonbirefrigent fluid phases (assumed to be isotropic liquids) at the temperatures that would have been expected from the DSC analysis. Additionally, no monotropic phases were observed on cooling, and no attempts at homeotropically aligning the samples were made to induce mesophases.

CONCLUSIONS

We have devised a strategy for the synthesis of carbazole containing banana-shaped mesogens by appealing to the double electrophilic aromatic substitution of the carbazole moiety at the 3 and 6 positions, to afford a carbazole unit which will act as a bend unit in banana-shaped mesogens. The crystal structure of the first in the series of compounds (**1a**) has established the structure has a significant bend (as does **1b**). The thermal analysis of these compounds reveals, that **1a-d** do not display any mesophase behaviour, but the DSC trace of **1e** reveal that this might be a mesophase forming material. However, optical polarised microscopy does not reveal any birefringent liquid. It is of no great surprise that this first generation of banana-shaped carbazole compounds have not afforded a mesophase given what is known currently about the structural units which are allowed in banana-mesogen chemistry. However, our chemical approach will allow various functionalities to be introduced at the 3,6-positions such that other mesogenic linking groups are now being incorporated in our laboratories, including esters and Schiff bases. Additionally, it is our intention to (i) N-methylate this series of compounds (**1a-f**) in order to remove the N-H···π hydrogen bond, which may prevent a mesophase from forming by effectively stopping formanistropic alignment of the molecules in the liquid phase, as well as (ii) N-alkylate in order to attempt to induce discotic mesophases.

As has already been noted[30] the stage of development of banana-shaped liquid crystals is reminiscent of the early stages of development of calamitic and

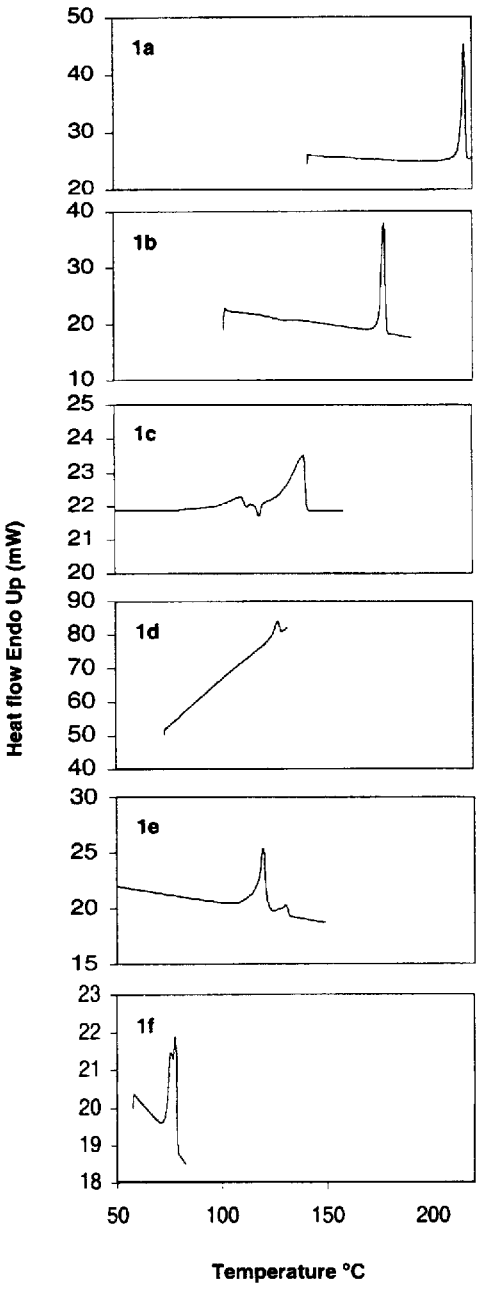

FIGURE 4 DSC Traces of compounds **1a-f**

discotic liquid crystals, such that slight changes in chemical structure have pronounced effects on whether a material exhibits a mesophase or not, and indeed what type of mesophase is adopted. Thus, the message is clear, research in this area of liquid crystals will be both challenging and rewarding.

EXPERIMENTAL SECTION

General

Commercially available chemicals were purchased from Aldrich and used as such without any further purification. Column chromatographic separations were performed on silica gel 60 (Merck 9385, 230–400 mesh and ICN 32–63 Mesh). Thin-layer chromatography (TLC) was carried out on aluminium sheets coated with silica gel 60 F_{254} (Merck 5554). ^{1}H-NMR spectra were recorded on a Bruker AC300 (300 MHz) spectrometer, ^{13}C-NMR spectra were recorded on a Bruker AC300 (75 MHz) spectrometer using the PENDANT pulse sequence. All chemical shifts are quoted in δ (ppm) to high frequency from Me_4Si, using deuterated acetone (acetone-d_6) or chloroform ($CDCl_3$) as the lock and the residual solvent as the internal standard. The coupling constants J are expressed in hertz (Hz) with multiplicities abbreviated as follows: s = singlet, d = doublet, t = triplet, m = multiplet, b = broad multiplet. Electron Impact Mass Spectrometry (EIMS) was performed on a VG ProSpec instrument, and Liquid Secondary Ion Mass Spectrometry (LSIMS) was performed on a VG ZabSpec instrument equipped with a cesium ion source. Optical polarising microscopy (OPM) experiments were carried out using an Olympus BX40 optical microscope with crossed polarisers equipped with a Linkam LT350 hot stage. Differential Scanning Calorimetry (DSC) results were recorded on a Perkin-Elmer 7 Series thermal analysis system. All samples were heated and cooled in a double cycle, at the rate of 10.00 °C/min.

The crystals used were grown by the vapour diffusion of hexane into a solution of **1a** and **1b** in EtOAc, respectively. Diffraction data were recorded on a Rigaku R-Axis IIc diffractometer equipped with an image plate detector system and a rotating anode source. Image plate scans were recorded covering 180° of crytal rotation in 4° frames about one axis with crystal-detector distance of 100 mm and exposure time of 50–60 minutes per frame. The crystal structure of **1a** is monoclinic, C2/c, with cell parameters a = 21.024(6), 6.0356(14), c = 31.529(8), β = 101.976(3). The crystal structure of **1b** is monoclinic $P2_1/c$ with cell parameters a = 18.533(6), b = 5.4489(14), c = 27.768(7), β = 99.140(4). The structures

were solved by direct methods[29] and refined using SHELX software.[30] Coordinates and anisotropic displacement parameters were refined for non-hydrogen atoms. All hydrogen atoms were placed in calculated positions, and the C-H bonds were normalised to 1.09Å for calculations. Final $R_1 = 6.62\%$ and $wR_2 = 15.79\%$ were obtained for **1a** and final $R_1 = 14.50\%$ and $wR_2 = 34.2\%$ were obtained for **1b**. Crystallographic data (excluding structure factors) for compounds **1a** and **1b** have been deposited with the Cambridge Crystallographic Data Centre as supplementary publication numbers CCDC 148665 and CCDC 150187, respectively. Copies of the data can be obtained free of charge on application to CCDC, 12 Union Road, Cambridge CB2 1EZ, UK (Fax: + 44 1223 336033 or email: deposit@ccdc.cam.ac.uk).

All calculations have been carried out using the MOPAC[31] program and AM1[32] hamiltonian. Optimised geometries have been characterised by frequency calculations and all geometries verified as true minimum energy conformations. Atomic charges were determined from the computed wavefunction using the ESP option[33] of Besler, Merz and Kollman and displayed using the program Grasp.[34]

3,6-Dibromocarbazole 2[35]

Carbazole (1.7 g, 10 mmol) was dissolved in a stirred slurry of silica gel (40 g) in anhydrous CH_2Cl_2 (200 mL). A solution of NBS (3.6 g, 20 mmol) in anhydrous CH_2Cl_2 (300 mL) was added dropwise. The reaction mixture was left stirring at room temperature, under a N_2 atmosphere and in the absence of light for 6 hours. The slurry was filtered and the silica washed with CH_2Cl_2 (3 × 50 mL). The combined extracts were washed with H_2O (100 mL) and brine (100 mL), dried ($MgSO_4$), filtered and the filtrate concentrated *in vacuo*. The crude product was repeatedly recrystallised from acetone and hexane to yield a blue-green crystalline solid 2.1 g (66%) of **2**. mp 206–208 °C (lit[35]mp 206–208 °C). ^{1}H-NMR (acetone-d_6): δ_H 7.51 (*d*, $J = 8.5$, 2H), 7.55 (*dd*, $J = 8.5$ and $J = 1.75$, 2H), 8.37 (*d*, $J = 1.75$, 2H), 10.71 (*bs*, 1H, NH); ^{13}C-NMR (acetone-d_6): δ_C 112.35, 113.76, 123.97, 124,70, 129.72, 139.95; *m/z* (EIMS): 325 $[M]^+$, 244 and 246 $[M\text{-}Br]^+$, 165 $[M\text{-}2Br]^+$.

3,6-Di-(para-methoxyphenyl)carbazole 1a

A solution of **2** (0.325 g, 1.0 mmol) and **3a** (0.365 g, 2.4 mmol) were dissolved in DME (20 mL) and stirred. Tetrakis(triphenylphosphine)palladium(0) (0.462 g, 0.4 mmol) was added to the mixture. An aqueous solution (20 mL) of sodium

hydrogen carbonate (2.5 g, 22.8 mmol) was added and the mixture was carefully deoxygenated by the freezing technique. The reaction mixture was heated to 80–85 °C under a N_2 atmosphere for 3 hours. The cooled mixture was poured into H_2O (100 mL) and the product extracted into Et_2O (2 × 100 mL). The combined organic layers were washed with brine (100 mL), dried ($MgSO_4$), filtered and the filtrate concentrated *in vacuo*. The crude product was purified by silica gel column chromatography (increasing the polarity of the eluent from 0 to 7.5% EtOAc in hexane). The chromatographic product was recrystallised from EtOAc and hexane to give a white amorphous solid 0.23 g (60%) of **1a**. Found C, 82.31; H, 5.41; N, 3.61. $C_{26}H_{21}NO_2$ expected C, 82.30; H, 5.58; N, 3.69; mp 214.6 °C; ^{1}H NMR (acetone-d_6): δ_H 3.8 (*s*, 6H), 7.05 (*m*, 4H), 7.57 (*d*, J = 8.1, 2H), 7.66–7.72 (*m*, 6H), 8.48 (*s*, 2H), 10.40 (*bs*, 1H); ^{13}C NMR (acetone-d_6): δ_C 55.48, 111.98, 114.95, 118.86, 124.69, 125.53, 128.67, 132.75, 135.32, 140.54, 159.57; *m/z* (EIMS): 379 $[M]^+$, 364 $[M\text{-}CH_3]^+$, 349 $[M\text{-}2CH_3]^+$.

3,6-Di-(para-alkoxyphenyl)carbazole 1b-1f

The same procedure for the synthesis of **1a** was followed for **1b-1f. Table I** lists the amount of reagents used. Analytical data for the series are listed in **Table II**.

TABLE I Quantities of reagents used to synthesise compounds **1b-1f**

Target	*2*	*Boronic acid*	*Pd(PPh$_3$)*	*Na$_2$CO$_3$*	*DME*	*H$_2$O*	*Yield*
1b	0.406 g,	**3b** 0.540 g,	0.685 g,	3.0 g,	25 ml	20 mL	0.272 g,
	1.25 mmol	3.0 mmol	0.6 mmol	28.7 mmol			50 %
1c	0.146 g,	**3c**: 0.197 g,	0.104 g,	0.540 g,	20 mL	20 mL	0.110 g,
	0.45 mmol	0.95 mmol	0.09 mmol	5.1 mmol			50 %
1d	0.208 g,	**3d**: 0.350 g,	0.400 g,	1.5 g,	20 mL	20 mL	0.096 g,
	0.6 mmol	1.5 mmol	0.35 mmol	14.3 mmol			28 %
1e	0.266 g,	**3e**: 0.480 g,	0.378 g,	2.0 g,	20 mL	20 mL	0.200 g,
	0.82 mmol	1.8 mmol	0.3 mmol	18.8 mmol			40 %
1f	0.271 g,	**3f**: 0.584 g,	0.381 g,	2.0 g,	25 mL	20 mL	0.291 g,
	0.8 mmol	2 mmol	0.3 mmol	18.8 mmol			53 %

para-Methoxybromobenzene 4a[36]

A solution of bromophenol (17.3 g, 0.1 mol) in MeCN (200 mL) was added to K_2CO_3 (138.0 g, 1.0 mol). The resultant slurry was stirred and heated under reflux for 0.5 hours under an N_2 atmosphere. A solution of MeI (14.2 g, 0.1 mol) in MeCN (50 mL) was added, dropwise over a few minutes to the slurry, maintaining reflux and stirring overnight. The reaction was cooled to room tempera-

ture and the inorganic residues were filtered off, and the filtrate concentrated *in vacuo*. The resulting oil was dissolved in Et_2O (20 mL) and washed with aqueous NaOH (2 M, 2 × 25 mL), and with H_2O (50 mL). The organic layer was separated, dried ($MgSO_4$), filtered and the filtrate concentrated *in vacuo* to yield 13.4 g (72 %) of a light yellow oil **4a**. ^1H NMR ($CDCl_3$): δ_H 3.72 (*s*, 3H), 6.72 (*d*, J = 8.8, 2H), 7.31 (*d*, J = 8.8, 2H); ^{13}C NMR ($CDCl_3$): δ_C 55.43, 112.77, 115.73, 132.23, 158.69; *m/z* (EIMS); 186 and 188 $[M]^+$.

para-Alkoxybromobenzene 4b-4f

The same procedure was followed as for the synthesis of **4a** for **4b-f**. Identical quantities of reagents were used, affording **4b** (16.6 g, 77%), **4c** (19.8 g, 82%), **4d** (20.7 g, 76%), **4e** (23.7 g, 79%), **4e** (23.3 g, 71%). Analytical data for **4b-4f** is shown in **Table III**.

para-Methoxyphenylboronic acid 3a[37]

A solution of **4a** (7.2 g, 38.7 mmol) in anhydrous THF (120 mL) was stirred and cooled to −78 °C (dry ice/acetone). BuLi (25.2 mL, 1.6 M solution in hexane, 40.5 mmol) was added under a N_2 atmosphere via a syringe through a septum. The reaction was left at −78 °C for 45 min. Trimethyl borate (4.6 mL, 40.5 mmol) was added to the mixture, via a syringe through a septum, maintaining the temperature at −78 °C for 1 h. The mixture was kept at room temperature overnight. The reaction was quenched with aqueous HCl (25 mL, 10 %) and stirred for a further 1 h. The aqueous layer was extracted with EtOAc (2 × 50 mL) and the combined organic layers were dried ($MgSO_4$), filtered, and the filtrate was concentrated *in vacuo*. The crude solid was purified by recrystallisation from H_2O to yield a white solid 3.3 g (57%) of **3a** as a mixture of the acid and anhydride. mp 204–206 °C. ^1H NMR ($CDCl_3$): acid δ_H 3.84 (*s*, 3H), 4.59 (*bs*, 2H), 6.93 (*d*, J = 8.6, 2H), 7.68 (*d*, J = 8.6, 2H); anhydride: δ_H 3.89 (*s*, 9 H), 7.01 (*d*, J = 8.6, 6 H), 8.16 (*d*, J = 8.6, 6 H); ^{13}C NMR ($CDCl_3$): δ_C 55.18, 113.52, 137.53, 163.18 (quaternary carbon atom resonance attached to boron atom was not observed. Anhydride ^{13}C NMR spectra is coincident with the acid spectra); acid *m/z* (EIMS) 152 $[M]^+$; anhydride: *m/z* (EIMS): 402 $[M]^+$.

para-Alkoxyphenylboronic acid 3b-3f

The same procedure was followed as for the synthesis of **3a** for the homologous compounds **3b-f**, with identical quantities of reagents. The only difference was for compounds **3c-3f** where a mixture of EtOAc/hexane was used as solvent for the recrystallisation. Analytical data for **3b-f** are listed in **Table IV** and for the anhydrides in **Table V**.

TABLE II Analytical data for compounds **1b-1f** (mp °C): δ_H (acetone-d_6), δ_C (acetone-d_6), *m/z* (EIMS), elemental analysis (EA) or High Resolution Mass Spectrometry (HRMS)

Target	*NMR*	*m/z*	*EA/HRMS*
1b mp 175.7°C	δ_H: 1.06 (*t*, *J* = 7.35, 6H), 1.82 (*m*, 4H), 4.01 (*t*, *J* = 6.6, 4H), 7.04 (*d*, *J* = 8.8, 4H), 7.57 (*d*, *J* = 8.45, 2H), 7.66-7.72 (*m*, 6H), 8.48 (*d*, *J* = 1.47, 2H), 10.40 (*bs*, 1H); δ_C: 10.71, 23.24, 69.98, 112.00, 115.53, 118.81, 124.71, 125.51, 128.54, 132.78, 135.20, 140.46, 159.04	435 $[M]^+$, 392 $[M\text{-}C_3H_7]^+$	HRMS Expected 435.2189 Found 435.2207
1c[a] mp 129.5°C	δ_H: 0.94 (*t*, *J* = 6.8, 6H), 1.37–151 (*m*, 8H), 1.83 (*m*, 4H), 4.02 (*t*, *J* = 6.6, 4H), 7.00 (*d*, *J* = 8.1, 4H), 7.47 (*d*, *J* = 8.4, 2H), 7.63 (*m*, 6H), 8.06 (*bs*, 1H), 8.27 (*bs*, 2H); δ_C: 14.01, 22.48, 28.25, 29.05, 68.15, 110.80, 114.85, 118.35, 124.04, 125.26, 128.19, 132.88, 134.50, 139.06, 158.22	491 $[M]^+$, 420 $[M\text{-}C_5H_{11}]^+$, 351 $[M\text{-}2C_5H_{10}]^+$	
1d mp 124.6°C	δ_H: 0.91 (*t*, *J* = 6.4, 6H), 1.34–1.56 (m, 16H), 1.77–1.86 (*m*, 4H), 4.06 (*t*, *J* = 6.6, 4H), 7.04 (*dd*, *J* = 3.3 and 11.8, 4H), 7.57 (*d*, *J* = 8.45, 2H), 7.66–7.73 (*m*, 6H), 8.48 (*bs*, 2H), 10.39 (*bs*, 1H), δ_C: 14.09, 23.01, 26.51, 32.30, 68.28, 111.76, 115.34, 118.62, 124.55, 125.32, 128.44, 132.60, 134.98, 140.27, 158.85	547 $[M]^+$, 449 $[M\text{-}C_7H_{14}]^+$, 351 $[M\text{-}2C_7H_{14}]^+$	HRMS Expected 547.3450 Found 547.3459
1e mp 127.2°C	δ_H: 0.89 (*t*, *J* = 6.9, 6H), 1.30–1.55 (*m*, 24 H), 1.75–1.84 (*m*, 4H), 4.04 (*t*, *J*= 6.4, 4H), 7.04 (*d*, *J* = 8.8, 4H), 7.56 (*d*, *J* = 8.1, 2H), 7.66–7.71 (*m*, 6H), 8.48 (*d*, *J* = 1.1, 2H), 10.39 (*bs*, 1H); δ_C: 14.34, 23.31, 26.82, 30.11, 30.19, 30.30, 32.61, 68.64, 122.05, 115.68, 118.88, 124.85, 125.59, 128.72, 132.92, 135.32, 140.65, 159.16, 159.16	603 $[M]^+$, 476 $[M\text{-}C_9H_{19}]^+$, 351 $[M\text{-}2C_9H_{18}]^+$	EA $C_{42}H_{53}NO_2$: Expected C, 83.54; H, 8.85; N, 2.32 C, 83.34, H, 8.56, N, 2.50
1f mp 77.7°C	δ_H: 0.88 (*t*, *J* = 6.1, 6H), 1.30–1.57 (*m*, 32H), 1.81 (*m*, 4H), 4.06 (*t*, *J* = 6.2, 4H), 7.04 (*d*, *J* = 8.5, 4H), 7.57 (*d*, *J* = 8.5, 2H), 7.66–7.72 (*m*, 6H), 8.48 (s, 2H), 10.39 (*bs*, 1H); δ_C: 14.37, 23.33, 26.81, 30.15, 30.33, 32.63, 68.55, 112.02, 115.61, 118.88, 124.79, 125.57, 128.71, 132.86, 135.23, 140.54, 159.12	659 $[M]^+$, 504 $[M\text{-}C_{11}H_{23}]^+$, 351 $[M\text{-}2C_{11}H_{21}]^+$	

a. $CDCl_3$ was the NMR solvent

TABLE III Analytical data for compounds **4b-f**, $\delta_H(CDCl_3)$; δ_C ($CDCl_3$); *m/z* (EIMS)

Target	*NMR*	*m/z*
4b	δ_H: 1.02 (*t*, *J* = 7.5, 3H), 1.73–1.85(*m*, 2H), 3.87 (*t*, *J* = 6.4, 2H), 6.76 (*d*, *J*= 8.8, 2H), 7.35 (*d*, *J* = 8.8, 2H); δ_C: 10.53, 22.53, 69.75, 112.58, 116.32, 132.22, 158.75	214 and 216 $[M]^+$, 172 and 174 $[M\text{-}C_3H_6]^+$
4c	δ_H: 0.92 (*t*, *J* = 6.8, 3H), 1.31–1.47 (*m*, 4H), 1.72- 1.81 (*m*, 2H), 3.90 (*t*, *J* = 6.2, 2H), 6.76 (*d*, *J* = 8.8, 2H), 7.35 (*d*, *J* = 8.8, 2H); δ_C: 14.09, 22.52, 28.22, 28.93, 68.30, 112.60, 116.35, 132.25, 158.31	242 and 244 ($[M]^+$), 172 and 174 $[M\text{-}C_5H_{10}]^+$
4d	δ_H: 0.88 (*t*, *J* = 6.4, 3H), 1.30–1.43 (*m*, 8H), 1.71- 1.81 (*m*, 2H), 3.90 (*t*, *J* = 6.6, 2H), 6.76 (*d*, *J* = 8.8, 2H), 7.35 (*d*, *J* = 8.8, 2H); δ_C: 14.13, 22.65, 25.99, 29.09, 29.21, 31.80, 68.28, 112.56, 116.31, 132.21, 158.27	270 and 272 $[M]^+$, 172 and 174 $[M\text{-}C_7H_{14}]^+$
4e	δ_H: 0.89 (*t*, *J* = 6.6, 3H), 1.28–1.46 (*m*, 12H), 1.72- 1.79 (*m*, 2H), 3.90 (*t*, *J* = 6.6, 2H), 6.76 (*d*, *J* = 8.8, 2H), 7.35 (*d*, *J* = 8.8, 2H); δ_C: 14.18, 22.74, 26.05, 29.23, 29.32, 29.45, 29.59, 31.93, 68.27, 112.57, 116.30, 131.82, 158.28	298 and 300 $[M]^+$, 172 and 174 $[M\text{-}C_9H_{18}]^+$
4f	δ_H: 0.88 (*t*, *J* = 6.6, 3H), 1.26–1.45 (*m*, 16H), 1.71- 1.80 (*m*, 2H), 3.90 (*t*, *J* = 6.4, 2H), 6.76 (*d*, *J* = 8.8, 2H), 7.35 (*d*, *J* = 8.8, 2H); δ_C: 14.12, 22.68, 25.97, 29.14, 29.32, 29.36, 29.54, 29.58, 29.59, 31.89, 68.46, 112.74, 116.49, 132.39, 158.45	326 and 328 $[M]^+$, 172 and 174 $[M\text{-}C_{11}H_{22}]^+$

TABLE IV Analytical data for compounds **3b-f** (as a mixture with the anhydride), δ_H[a] ($CDCl_3$); δ_C[b]($CDCl_3$); melting point; *m/z* (EIMS **3b-3d** or LSIMS **3e-3f**)

Target	*NMR*	*m/z*
3b mp 130°C	δ_H: 3.95 (*t*, *J* = 6.6, 2H), 4.50 (*bs*, 2H), 6.92 (*d*, *J* = 8.5, 2H), 7.66 (*d*, *J* = 8.5, 2H); δ_C: 10.60, 22.63, 69.33, 113.70, 137.52, 162.77	180 $[M]^+$, 138 $[M\text{-}C_3H_6]^+$
3c mp 106–107°C	δ_H: (*t*, *J* = 6.6, 2H), 4.49 (*bs*, 2H), 6.92 (*d*, *J* = 8.8, 2H), 7.66 (*d*, *J* = 8.8, 2H); δ_C: 14.59, 22.48, 28.20, 28.92, 67.84, 113.97, 137.45, 162.76	208 $[M]^+$, 138 $[M\text{-}C_5H_{10}]^+$
3d mp 96.5°C	δ_H: 3.98 (*t*, *J* = 6.6, 2H), 4.50 (*bs*, 2H), 6.92 (*d*, *J* = 8.8, 2H), 7.66 (*d*, *J* = 8.8, 2H); δ_C: 14.10, 22.62, 26.01, 29.09, 29.23, 31.79, 67.85, 113.96, 137.45, 162.75	236 $[M]^+$, 138 $[M\text{-}C_7H_{14}]^+$
3e mp 92 °C	δ_H: 3.98 (*t*, *J* = 6.6, 2H), 4.53 (*bs*, 2H), 6.92 (*d*, *J* = 8.7, 2H), 7.65 (*d*, *J* = 8.7, 2H); δ_C: 14.12, 22.67, 26.04, 29.27, 29.41, 29.54, 31.87, 56.00, 67.87, 113.97, 137.45, 162.76	534[c] $[M+2NOBA\text{-}2H_2O]^+$, 138 $[M\text{-}C_9H_{18}]^+$
3f mp 83–85 °C	δ_H: 4.00 (*t*, *J* = 6.5, 2H), 4.55 (*bs*, 2H), 6.93 (*d*, *J* = 8.6, 2H), 7.67 (*d*, *J* = 8.6, 2H); δ_C: 15.26, 22.69, 26.04, 29.34, 29.41, 29.57, 29.60, 31.90, 56.01, 65.86, 67.87, 113.98, 137.45, 162.77	562[c] $[M+2NOBA\text{-}2H_2O]^+$

a. Mixture of acid and anhydride.

b. Quaternary carbon resonance attached to boron was not observed.

c. NOBA (nitrobenzyl alcohol) is present in the LSIMS matrix.

TABLE V Analytical data for the anhydrides (as a mixture with the respective acids **3b-f**), δ_H ($CDCl_3$); *m/z* (EIMS)

Target	*NMR*	*m/z*
3b anhydride	δ_H: 1.07 (*t*, *J* = 7.3, 9H), 1.80–1.91 (*m*, 6H), 4.00 (*t*, *J* = 6.6, 6H), 7.00 (*d*, *J* = 8.5, 6H), 8.15 (*d*, *J* = 8.5, 6H)	486 $[M]^+$, 360 $[M\text{-}C_9H_{18}]^+$
3c anhydride	δ_H: 0.95 (*t*, *J* = 7.5, 9H), 1.35–1.53 (*m*, 12H), 1.78- 1.88 (*m*, 6H), 4.00 (*t*, *J* = 6.6, 6H), 6.99 (*d*, *J* = 8.8, 6H), 8.15 (*d*, *J* = 8.8, 6H)	570 $[M]^+$, 360 $[M\text{-}C_{15}H_{30}]^+$
3d anhydride	δ_H: 0.90 (*t*, 9H), 1.34–1.51 (*m*, 24H), 1.78–1.87 (*m*, 6H), 4.03 (*t*, *J* = 6.6, 2H), 6.99 (*d*, *J* = 8.5, 6H), 8.14 (*d*, *J* = 8.5, 6H)	655 $[M]^+$, 360 $[M\text{-}C_{21}H_{42}]^+$
3e anhydride	δ_H: 0.88–0.92 (*t*, 9H), 1.30–1.50 (*m*, 36H), 1.78–1.85 (*m*, 6H), 4.05 (*t*, *J* = 6.6, 6H), 7.00 (*d*, *J* = 8.6, 6H), 8.15 (*d*, *J* = 8.6, 6H)	738 $[M]^+$, 360 $[M\text{-}C_{27}H_{54}]^+$
3f anhydride	δ_H: 0.89 (*t*, *J* = 6.71, 9H), 1.28–1.50 (*m*, 48H), 1.77- 1.86 (*m*, 6H), 4.05 (*t*, *J* = 6.5, 6H), 7.00 (*d*, *J* = 8.6, 6H), 8.15 (*d*, *J* = 8.6, 6H)	822 $[M]^+$, 360 $[M\text{-}C_{33}H_{66}]^+$

Acknowledgements

This research is supported by an EPSRC project studentship (MB), Leverhulme Trust (MM) and Perkin-Elmer/EPSRC in the UK through the Joint Research Equipment Initiative (JREI).

References

[1] (a) J.T. Link, S. Raghavan, M. Gallant, S. Danishefsky, T.C. Chou, L.M. Ballas, *J. Am. Chem. Soc.* **118**, 2825 (1996).
(b) Y. Yamashita, N. Fujii, C. Murkata, T. Ashiawa, M. Okabe, H. Nakano, *Biochemistry* **31**, 12069 (1992). (c) D.P. Chakraborty, *Prog. Chem. Org. Nat. Prod.* Vol. 34.

[2] Y. Zhang, T. Wada, H. Sasabe, *J. Mater. Chem.* **8**, 809 (1998).

[3] The space charge field induced photorefractive effect was first observed in inorganic electro-optic $LiNbO_3$ crystals by A. Ashkin, G.D. Boyd, J.M. Dziedic, R.G. Smith, A. A Ballman, K. Nassau, *Appl. Phys. Lett.* **9**, 72 (1966).

[4] The first report of a carbazole containing photorefractive material was by Y. Zhang, Y. Cui, P.N. Prasad, *Phys. Rev. B* **46**, 9900 (1992).

[5] P. Günter, J.-P. Huignardm, Eds *Photorefractive Materials and Their Applications*; Springer-Verlag, New York, 1988. For example of holographic application see; M.D. Rahn, D.P. West, J.D. Shakos, *J. Appl. Phys.* **87**, 627 (2000).

[6] S. Maruyama, X.-t. Tao, H. Hokari, T. Noh, Y. Zhang, T. Wada, H. Sasabe, T. Watanabe, S. Miyata, *J. Mater. Chem.* **9**, 893 (1999). For a related a related topic on fluorescent LEDs see; M.A. Baldo, M.E. Thompson, S.R. Forest, *Nature* **403**, 750 (2000).

[7] Y. Zhang, L. Wang, T. Wada, H. Sasabe, *Chem. Commun.* **559** (1996).

[8] J.C. Scott, L. Th. Pautmeier, W.E. Moerner, *J. Opt. Soc. Am. B* **9**, 2059 (1992).

[9] The first report of an amorphous organic photorefractive material was by S. Ducharme, J.C. Scott, R.J. Twieg, W.E. Moerner, *Phys. Rev. Lett.* **66**, 1846 (1991).

[10] K. Sutter, J. Hulliger, P. Günter, *Solid State Chem.* **74**, 867 (1990).

[11] Y. Zhang, T. Wada, L. Wang, H. Sasabe, *Chem. Mater.* **9**, 2798 (1997).

[12] The carbazole moiety has been introduced into a low molecular weight calamitic mesogenic structures which diplays a nematic mesophase, see M. Lux, P. Strohriegl, *Makromol. Chem.* **188**, 811(1987).

[13] B. Marcher, L. Chapoy, D.H. Christensen, *Macromolecules* **21**, 677 (1988).

[14] D. Demus, J. Goodby, G.W. Gray, H.-W. Speiss, V. Vill, (eds), 1998, *Handbook of Liquid Crystals vol. 2B*(Weinheim: Wiley-VCH) pp 693–780.

[15] R.B. Meyer, *Mol. Cryst. Liq. Cryst.* **40**, 33 (1977).

[16] For the first report regarding bent shaped mesogens and their modification to smectic phases see; T. Niori, T. Sekine, J. Watanabe, T. Furukawa, H. Takezoe, *J. Mater. Chem.* **6**, 1231–1233 (1996). However, it is interesting to note that Vorlander and Apel synthesised bent shaped mesogens back in 1929, see; D. Vorlander, *Ber. Dtsch. Chem. Ges.* **63**, 2831 (1929) and D. Vorlander, A. Apel, *Ber. Dtsch. Chem. Ges.* **65**, 1101 (1932). Additionally, Akutagawa published four bent compounds in 1994 which exhibited smectic mesophases but no structural peculiarties were noted, see; T. Akutagawa, Y. Matsunaga, K. Yasuhara, *Liq. Cryst.* **17**, 659 (1994). The term banana for the description of the molecular shape has evolved from the fact that the first bent mesogens had flexible linkers around a bent 1,3-substituted benzene moiety and were qualified as being statistically bent, see for example;
(a) D. Shen, S. Diele, G. Pelz, I. Wirth, C. Tschierske, *J. Mater. Chem.* **9**, 661 (1999).
(b) A.S. Matharu, C. Grover, L. Kmoitov, G. Andersson, *J. Mater. Chem.* **10**, 1303, (2000) whilst some later structures had much more rigid bent molecular motifs and were referred to as boomerang shaped mesogens, see for example; T.J. Dingemans, E.T. Samulski, *Liq. Cryst.* **27**, 131 (2000).

[17] Ferroelectric liquid crystals were first postulated and observed in chiral mesogenic structures that induced polar ordering, see
(a) R.B. Meyer, L. Liebert, L. Strzelecki, P. Keller, *J. Phys. Lett.* **36**, L-69, (1975);
(b) N.A. Clarke, S.T. Lagerwall, *Appl. Phys. Lett.* **38**, 899 (1980). Later banana-shaped mes-

ogens were also shown to exhibit ferroelectric behaviour, see (a) T. Niori, T. Sekine, J. Watanabe, T. Furukawa, H. Takezoe, *J. Mater. Chem.* **6**, 1231 (1996) for the first report and (b) D.M. Walba, E. Körblova, R. Shao, J.E. Maclennan, D.R. Link, M.A. Glaser, N.A. Clark, *Science* **288**, 2181–2184 (2000) for a recent report.

[18] M. Manickam, S. Kumar, J.A. Preece, N. Spencer, *Liq. Cryst.* **27**, 703 (2000).

[19] T. Sekine, T. Niori, M. Sone, J. Watanabe, S.W. Choi, Y. Takanishi, H. Takezoe, *Jpn J. Appl. Phys.* **36**, 6455 (1997).

[20] G. Pelzl, S. Diele, A. Jakli, C. Lischka, I. Wirth, W. Weissflog, *Liq. Cryst.* **26**, 135 (1999).

[21] D. Shen, S. Diele, G. Pelzl, I. Wirth, C. Tschierske, *J. Mater. Chem.* **6**, 661 (1999).

[22] D. Shen, S. Diele, I. Wirth, C. Tschierske, *Chem. Commun.* 2573 (1998).

[23] G. Pelzl, S. Diele, S. Grande, A. Jakli, C. Lischka, H. Kresse, H. Schmalfuss, I. Wirth, W. Weissflog, *Liq. Cryst.* **26**, 401 (1999).

[24] I.A. Levitsky, K. Kishikawa, S.H. Eichhorn, T.M. Swager, *J. Am. Chem. Soc.* **122**, 2474 (2000).

[25] W. Weissflog, C. Lischka, I. Benne, T. Scharf, G. Pelzl, S. Diele, H. Kruth, *Proc. SPIE: Int. Soc. Opt. Eng.* **3319**, 14 (1998).

[26] For literature on X-H···π hydrogen bonds, see: a) S.E. Biali, Z. Rappoport, *J. Am. Chem. Soc.* **106**, 5641(1984); b) M.G.B. Drew, G.R. Willey, *J. Chem. Soc. Perk. Trans. 2*, 215–220 (1986); c) H.S. Rzepa, M.L. Webb, A.M.Z. Slawin, D.J. Williams, *J. Chem. Soc., Chem. Commun.*, 765–768(1991); D.A. Rodham, S. Suzuki, R.D. Suenram, F.J. Lovas, D. Dasgupta, G.A. Blake, *Nature* **362** (1993), 735–737; d) H. Adams, K.D.M. Harris, G.A. Hembury, C.A. Hunter, D. Livingston, J.M. McCabe, *Chem. Commun.*, 2351–2352 (1996); e) A.P. Bisson, V.M. Lynch, M.K.C. Monahan, E.V. Anslyn, *Angew. Chem. Int. Ed. Engl.* **36**, 2340–2342 (1997).

[27] V.K. Bel'skii, *Kristallografiya* **30**, 193 (1985).

[28] For an excellent review on banana-shaped liquid crystalline materials see; G. Pelz, S. Diele, W. Weissflog, *Adv. Mater.* **11**, 707 (1999).

[29] Molecular Structure Corporation (1993). TEXSAN. Single Crystal Structure Analysis Software. Version 1.6. MSC, 3200 Research Forest Drive, The Woodlands, TX 77381, USA.

[30] Sheldrick, G.M. (1993). SHELXL92. Program for the Refinement of Crystal Structures. University of Gottingen, Germany.

[31] J.J.P. Stewart. *Mopac VI*. QCPE #455.

[32] M.J.S. Dewar, E.G. Zoebisch, E.F. Healy, J.J.P. Stewart. *J. Am. Chem. Soc.* **107**, 3902–3909 (1985).

[33] B.H. Besler, K.M. Merz, Jr., P.A. Kollman, *J. Comp. Chem.* **11**, 431–439 (1990).

[34] A. Nichols, K. Sharp, B. Honig. *Proteins: Structure, Function and Genetics* **11**, 281 (1991).

[35] K. Smith, D.M. James, A.G. Mistry, M.R. Bye and D.J. Faulkner, *Tetrahedron* **48**, 7479–7488 (1992).

[36] W.G. Dauben, H. Tilles, *J. Am. Chem. Soc.* **72**, 3185–3187 (1950).

[37] W. Konig, W. Scharrnbeck, *J. Prakt. Chem.* 153–170 (1930).